COMPARISON OF ORSAT AND SCARAB REENTRY SURVIVAL RESULTS

T. Lips[1], **V. Wartemann**[1], **G. Koppenwallner**[1], **H. Klinkrad**[2], **D. Alwes**[3],
J. Dobarco-Otero[4], **R.N. Smith**[4], **R.M. DeLaune**[4], **W.C. Rochelle**[4], **and N.L. Johnson**[5]

[1]Hypersonic Technology Göttingen, Max-Planck-Str. 19, 37191 Katlenburg-Lindau, Germany, t.lips@htg-hst.de
[2]European Space Operations Center, ESA/ESOC, Darmstadt, Germany
[3]DLR (German Aerospace Center), Bonn, Germany
[4]Jacobs Sverdrup (ESCG), 2224 Bay Blvd., Houston, TX 77058, USA, jose.dobarcootero@escg.jacobs.com
[5]NASA Johnson Space Center, Houston, TX 77058, USA

ABSTRACT

The two reentry analysis tools, NASA ORSAT (Object Reentry Survival Analysis Tool) and ESA SCARAB (Spacecraft Atmospheric Reentry and Aerothermal Breakup), are standard codes for the reentry survivability assessment of decaying satellites. These programs determine if and when an object/fragment demises during reentry. The final debris casualty area caused by the surviving objects/fragments is calculated, which is used to determine the reentry risk posed to the Earth's population.

A set of test cases for both tools has been defined which comprises random tumbling or spinning simple geometric shapes (spheres, boxes, and cylinders), consisting of three materials (aluminum, titanium, and graphite epoxy composite). Geometric dimensions, wall thickness, and mass are varied, with the initial orbit conditions kept constant for each case. Both tools use the U.S. Standard 1976 atmosphere model and the same physical material properties.

This paper presents the main results of both tools and summarizes the discovered differences.

1. INTRODUCTION

Risk of debris from uncontrolled re-entries cannot be ignored. In the recent past, one person has been hit with a light piece of debris and fortunately was not hurt. Objects have re-entered and landed near residences. As a consequence, NASA and ESA have funded development of numerical tools that asses the re-entry risk of satellites during their design phase and/or prior to their re-entry.

The SCARAB software system (Spacecraft Atmospheric Re-Entry and Aerothermal Break-up) was developed for ESA by a group of contractors led by Hypersonic Technology Göttingen (HTG). In the hypersonic flow regime ($Ma > 6$) the trajectory is predicted by a numerical integration of the 6 degrees-of-freedom (DOF) equations of motion for an oblate Earth. For $Ma < 6$ only the 3-DOF equations are taken into account. In continuum flow the aerodynamic and aerothermodynamic models are based on modified Newtonian theory and modified Lees theory, respectively. In the free-molecular flow, Nocilla or Schaaf-Chambre accommodation coefficients are used. The thermal math model is based on 2-dimensional (2-D) heat conduction model. The thermal analysis stops at the hypersonic limit (Lips et al., 2004).

The Object Reentry Survival Analysis Tool (ORSAT) was developed jointly by NASA and Lockheed Martin. The 3-DOF equations of motion for a spherical Earth are solved with a 4th order Runge-Kutta numerical integration scheme. The drag force in equations of motion is dependent on the drag coefficient. The drag coefficient is a function of the shape of the object, the motion, and flow regime. In continuum flow the Detra-Kemp-Riddell equation is used to estimate the cold-wall stagnation heat rate for a sphere. In free molecular flow, the stagnation heat rate of a sphere is one-half the density times the velocity cubed multiplied by an accommodation factor of 0.9. Heating factors based on the shape and motion adjust the heat rate an object receives. The thermal response is predicted by a lumped or 1-D thermal math model (Lips et al., 2004).

A study performed in 1998/99 with a test matrix that consisted of only spheres yielded good results between ORSAT and SCARAB (Klinkrad, 1998; Rochelle et al., 1999). A similar study of a satellite by both codes produced differences in the final results.

The present comparison between ORSAT and SCARAB is performed using the U.S. Standard 1976 atmosphere with a test matrix that consists of random tumbling spheres, cylinders, and boxes for uncontrolled reentries. Furthermore, in the present study the same drag coefficients for spheres in both ORSAT and SCARAB are used (Koppenwallner, 1985). The materials used in the study are aluminum, titanium, and graphite epoxy. The proper-

Proceedings of the Fourth European Conference on Space Debris, Darmstadt, Germany, 18-20 April 2005
(ESA SP-587, August 2005)

ties of these materials in both codes were identical, and oxidation heating was not considered. The properties of graphite epoxy can be seen in Tab. 1. There is some uncertainty in the way a composite material such as graphite epoxy melts; hence two sets of properties were considered. The first set of properties assumes an ablator with a very large heat of fusion, while the second set assumes that the material will "char" when the "melting" temperature has been reached. The properties of the other materials are from previous comparisons (Rochelle et al, 1999). The initial conditions can be seen in Tab. 2. The physical properties of the cases in the present study can be seen in Tabs. 3 (spheres) and 4 (cylinders). The dimensions shown in Tab. 4 are for cylinder with a length/diameter (L/D) equal to 2. Similar cases were performed for length/width (L/W) equal to 2 for boxes and an L/D and L/W equal to 5 for cylinders and boxes, respectively. As a result, all boxes have a width equal to the diameter for the corresponding cylindrical cases. Also, in all boxes, the height and the width are equal. Cases 1-9B in Tabs. 3 and 4 have a variable mass, while the remaining cases have a constant mass. Therefore, a total of 120 cases were compared between both codes: 24 spheres, 48 cylinders and 48 boxes.

Table 1. Material properties of graphite epoxy.

Material	C_p [J/kg-K]	K [W/m-K]	ρ [kg/m^3]	ε [-]	h_f [J/kg]	T_m [K]
Gr Ep I	1100	110	1570	0.86	$16 \cdot 10^6$	700
Gr Ep II	879	0.9-6.4	1550.5	0.9	236	700

Table 2. Initial conditions of study.

Altitude	122,000 m
Relative Velocity	7410 m/s
Relative Flight Path Angle	-0.1°
Orbital Inclination	28°
(Latitude, Longitude)	(0°, 0°)

2. RESULTS

A summary of the results can be seen in Figs. 1 and 2 for all cases in which both ORSAT and SCARAB predicted demise for 44 (mostly aluminum and graphite epoxy II) cases or survival of the object for 71 (mostly all titanium and graphite epoxy I) cases, respectively. It can be seen that the coefficient of determination, R^2, is very good (close to 1). The coefficient of determination is a statistic parameter that explains how much of the variability in the variable in the ordinate can be explained by the fact that it is related to the variable in the abscissa, (i.e., how close the points are to the trend line). If the models predicted completely identical results, all points would lie along a 45-degree trend line ($y = x$, $R^2 = 1$). On average, for the demise altitude, the deviations and the scattering are greater than for the impact mass. The mean deviation between both tools for the surviving mass is smaller than 0.2%.

Table 3. Physical properties for spheres in the study.

Case	Material	Outer Radius [m]	Inner Radius [m]	Mass [kg]
1	Al	0.125	0.075	17.318
2	Ti	0.125	0.075	28.222
3A	Gr Ep I	0.125	0.075	10.070
3B	Gr Ep II	0.125	0.075	9.945
4	Al	0.250	0.212	69.272
5	Ti	0.250	0.212	112.888
6A	Gr Ep I	0.250	0.212	40.280
6B	Gr Ep II	0.250	0.212	39.780
7	Al	0.500	0.465	276.459
8	Ti	0.500	0.465	450.525
9A	Gr Ep I	0.500	0.465	160.756
9B	Gr Ep II	0.500	0.465	158.759
10	Al	0.125	0.094	12.685
11	Ti	0.125	0.108	12.685
12A	Gr Ep I	0.125	0.029	12.685
12B	Gr Ep II	0.125	0.000	12.685
13	Al	0.250	0.244	12.685
14	Ti	0.250	0.246	12.685
15A	Gr Ep I	0.250	0.239	12.685
15B	Gr Ep II	0.250	0.239	12.685
16	Al	0.500	0.499	12.685
17	Ti	0.500	0.499	12.685
18A	Gr Ep I	0.500	0.498	12.685
18B	Gr Ep II	0.500	0.498	12.685

Five cases are not shown in either plot because either one model predicted survival and the other predicted demise (2 cases) or one model was unable to complete the calculation (3 cases). For example, in case 1 for a sphere, ORSAT predicted that the object would demise at 57.8 km, while SCARAB predicted that it would survive with a mass of 0.01 kg.

Fig. 3 plots the altitude vs. relative velocity for a surviving sphere and box, respectively. It can be seen that the profiles predicted by ORSAT and SCARAB are in excellent agreement. This trend can also be seen in boxes as well as cylinders. However, when the altitude is plotted against time, a large discrepancy exists in the profile for surviving objects. This can be seen in Fig. 4. This trend is seen in all shapes analyzed, and further investigations have shown that it becomes more pronounced for shallow initial path angles. However, this seems to be only a time effect (delayed SCARAB results in comparison with ORSAT) without any remarkable influence on the magnitude of the results.

At first, this difference was suspected to be attributed to the way the Earth is modeled. As ORSAT 5.8 uses a spherical Earth, whereas SCARAB uses an oblate Earth, due to decreasing radius of the Earth in the direction of the poles, objects in SCARAB would stay at a high geodetic altitude with increasing latitude where there is

Table 4. Physical properties of cylinders, $L/D = 2$.

Case	Material	Outer Radius [m]	Inner Radius [m]	Mass [kg]
1	Al	0.125	0.075	47.183
2	Ti	0.125	0.075	76.890
3A	Gr Ep I	0.125	0.075	27.436
3B	Gr Ep II	0.125	0.075	27.095
4	Al	0.250	0.209	188.731
5	Ti	0.250	0.209	307.562
6A	Gr Ep I	0.250	0.209	109.744
6B	Gr Ep II	0.250	0.209	108.381
7	Al	0.500	0.462	754.925
8	Ti	0.500	0.462	1230.248
9A	Gr Ep I	0.500	0.462	438.975
9B	Gr Ep II	0.500	0.462	433.523
10	Al	0.125	0.115	12.685
11	Ti	0.125	0.119	12.685
12A	Gr Ep I	0.125	0.106	12.685
12B	Gr Ep II	0.125	0.106	12.685
13	Al	0.250	0.248	12.685
14	Ti	0.250	0.249	12.685
15A	Gr Ep I	0.250	0.246	12.685
15B	Gr Ep II	0.250	0.246	12.685
16	Al	0.500	0.499	12.685
17	Ti	0.500	0.500	12.685
18A	Gr Ep I	0.500	0.499	12.685
18B	Gr Ep II	0.500	0.499	12.685

less drag because the atmosphere is less dense. But further comparisons with ORSAT 6.0 (not yet released), which models the oblateness of the Earth, also showed the observed differences. Thus, these differences are still under investigation.

The variation of Knudsen number and drag coefficient variation can be seen in Figs. 5 and 6, respectively. These figures show an excellent agreement. The Knudsen number determines whether the continuum flow assumption is appropriate and the amount of rarefied flow. The drag coefficient affects the drag force an object sees during reentry.

The predicted hot-wall stagnation heat rate for spheres and cylinders by ORSAT and SCARAB can be seen in Figs. 7 and 8, respectively. These plots are for surviving objects as opposed to demising objects. There is good agreement between both models for the peak values. The variation in time is due to the trajectory differences alluded to earlier. In both models, the heat rate increases slowly, abruptly rises, reaching peak heating, and suddenly decreases as the object's velocity has decreased and is about to hit the ground. The comparison of both models for two cylinders that demised can be seen in Fig. 9. The hot-wall stagnation heating rate predicted by SCARAB is not a smooth line because the stagnation condition is changing randomly with the orientation of the cylinder. Due to the geometry of sphere, the orientation does not change, and the heating rate predicted is smooth. In Figs. 8 and 9, the curves for the cylinders have

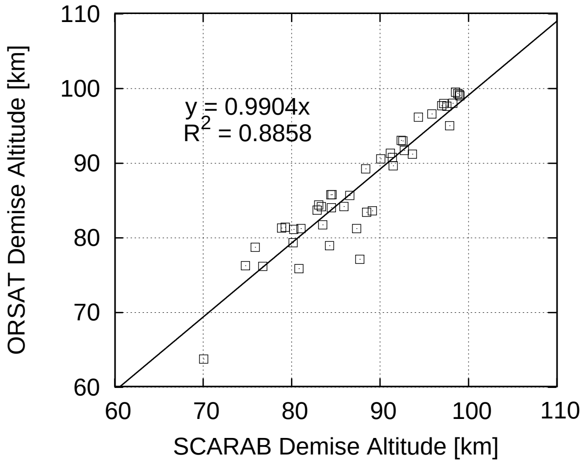

Figure 1. Comparison of demise altitude predicted by ORSAT and SCARAB for each case.

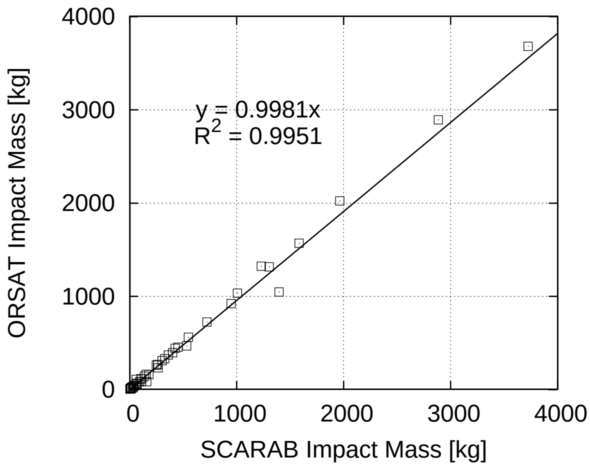

Figure 2. Comparison of impact mass predicted by ORSAT and SCARAB for each case.

been smoothed in order to achieve a clearer comparison with the ORSAT results.

The uniform average net heating rate vs. time for various spheres is shown in Fig. 10. The two graphite epoxy I cases show good agreement for the peak values, while the titanium case shows bigger differences (about 25% higher peak value in SCARAB). The time differences are again caused by the different trajectories.

The maximum surface temperature vs. time profiles of several cylinders and boxes can be seen in Figs. 11 and 12, respectively. All aluminum cases shown demised shortly after the melt temperature of 850 K was reached, and all titanium cases survived. In the titanium case the peak temperature of cylinders for both models are about the same, whereas in boxes, ORSAT predicts a lower peak temperature. The time at which the peak occurs is different due to differences in the trajectory.

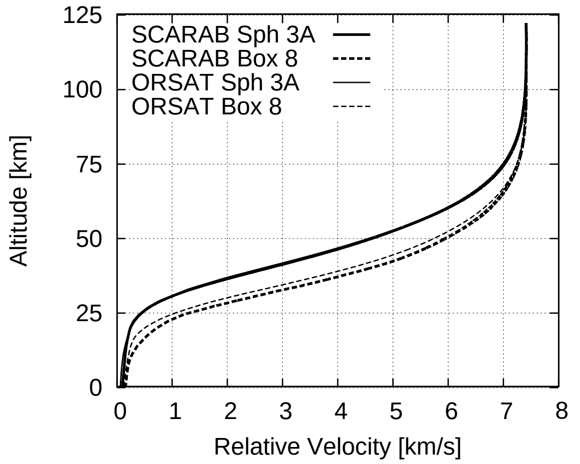

Figure 3. Altitude vs. relative velocity for two surviving cases.

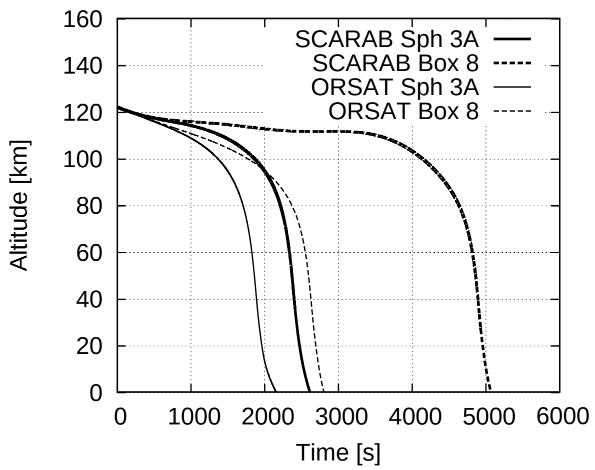

Figure 4. Altitude vs. time profile for two surviving cases.

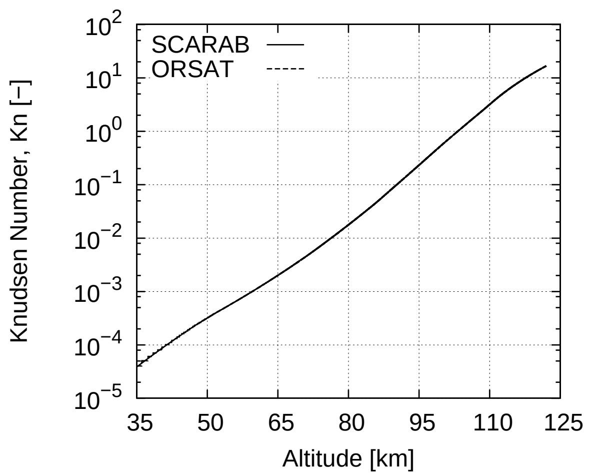

Figure 5. Knudsen number variation with altitude for Sphere Case 12A.

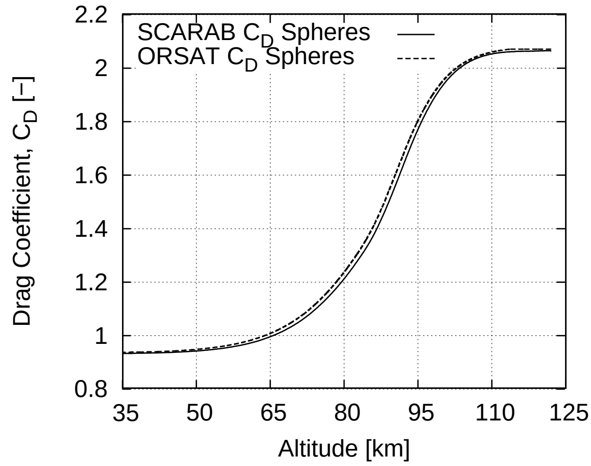

Figure 6. Drag coefficient variation with altitude for a sphere.

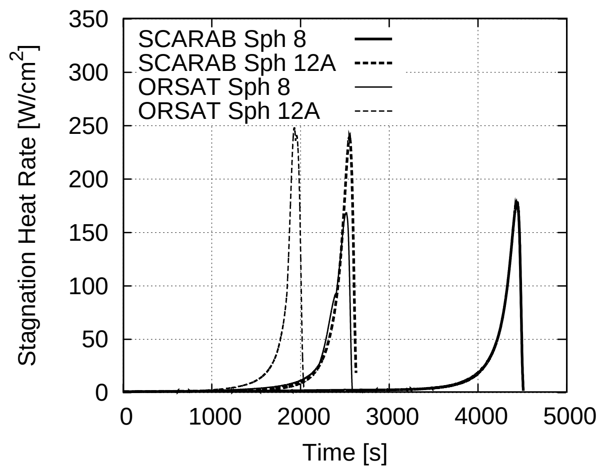

Figure 7. Hot-wall stagnation heat rate for two (graphite epoxy I and titanium) spheres that survived.

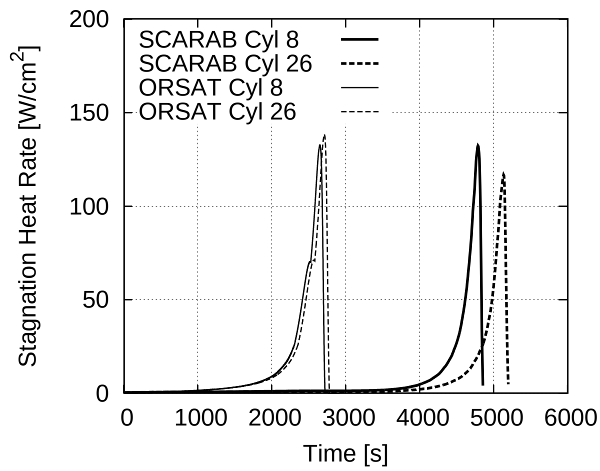

Figure 8. Hot-wall stagnation heat rate for two (titanium) cylinders that survived.

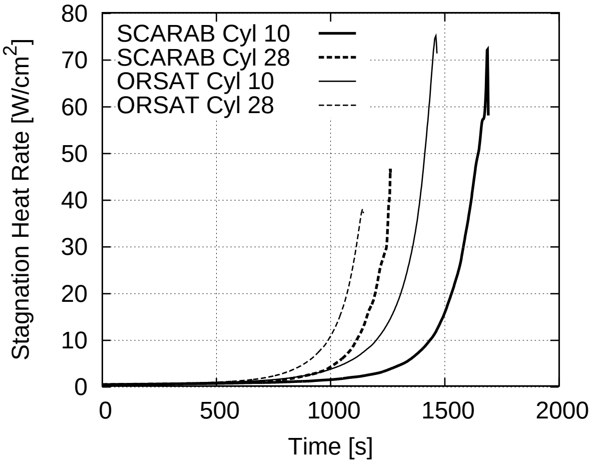

Figure 9. Hot-wall stagnation heat rate for two (aluminum) cylinders that demised.

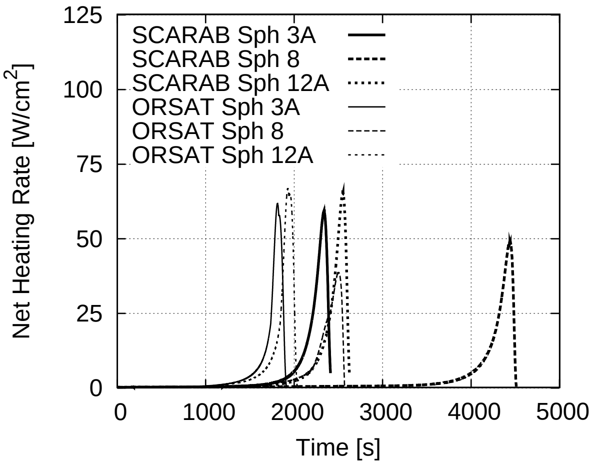

Figure 10. Average Net Heating Rate vs. time for various spheres.

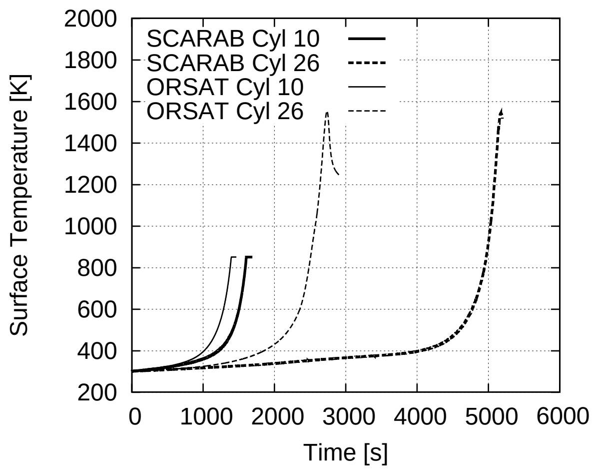

Figure 11. Maximum surface temperature vs. time for two cylinder cases.

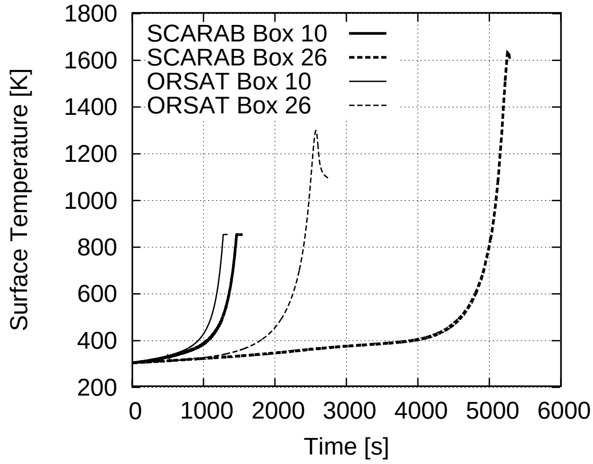

Figure 12. Maximum surface temperature vs. time for two box cases.

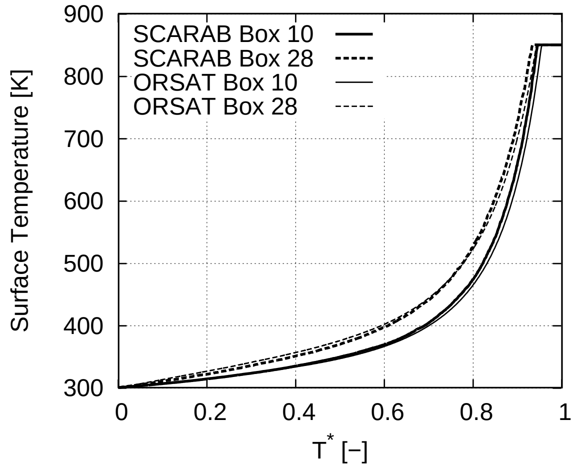

Figure 13. Max. surface temperature vs. non-dimensional time for demising aluminum boxes.

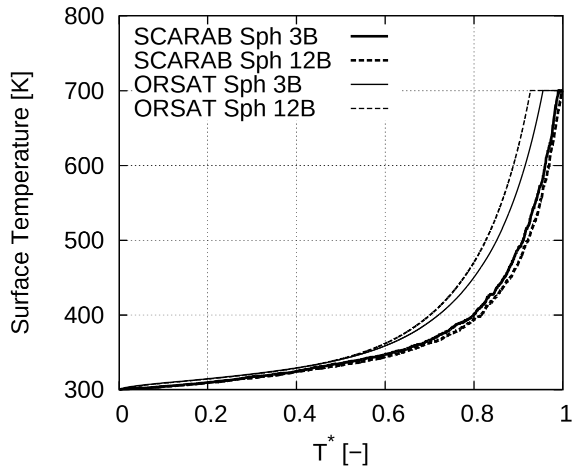

Figure 14. Max. surface temperature vs. non-dimensional time for demising graphite epoxy II spheres.

The differences in trajectory can be limited in the temperature response by plotting the maximum surface temperature against T^*, which is the current time divided by the time at which the object demised. The results can be seen in Figs. 13 and 14. In these figures it can be seen that the aluminum cases compare extremely well, (in fact it is almost an identical response), while the graphite epoxy II cases show some differences in the transient thermal response. Also, in SCARAB the graphite epoxy II objects demise rapidly as they reach the assumed melting temperature of 700 K, while in ORSAT it takes longer for all layers to ablate completely.

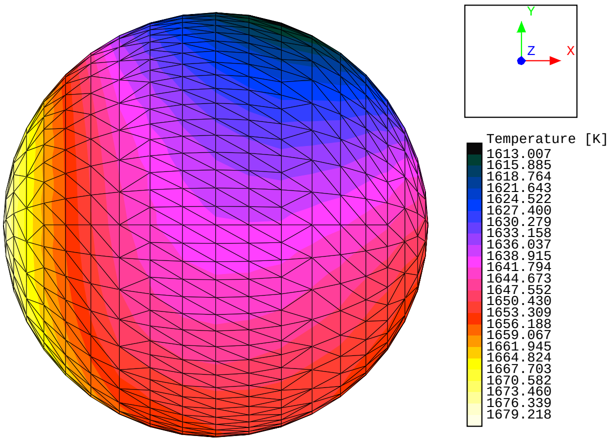

Figure 15. Temperature distribution of a titanium sphere.

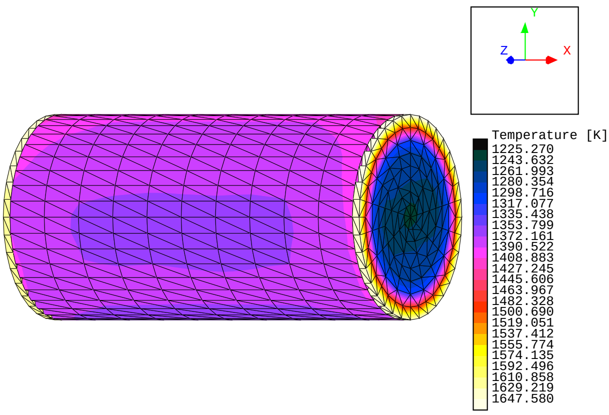

Figure 16. Temperature distribution of a titanium cylinder.

In ORSAT, the heat rates are averaged throughout the surface, so the surface temperature is constant. However, SCARAB calculates local heat fluxes, and as a result, the temperature is not constant even for a random tumbling sphere or cylinder as seen in Figs. 15 and 16, respectively. In the case of the sphere the temperature difference could be greater than 60 K, and in case of the cylinder even greater than 400 K.

3. CONCLUSIONS

The comparison study between SCARAB and ORSAT 5.8 revealed that the results are in good overall agreement as reflected by the high coefficients of determination of demising and surviving cases. The mean deviation between both tools for the surviving mass is smaller than 0.2%. This is an important fact for the use of SCARAB and ORSAT results for the purpose of on-ground risk assessments as they can be used with a high level of confidence.

It is remarkable that both tools show such good agreement for simple shape objects. As ORSAT and SCARAB use completely different approaches for the calculation of drag coefficients and heating rates (averaged shape dependent properties vs. local panel methods) this study can be considered as a cross-code validation for both tools.

The trajectory response differences are still under investigation. The resulting influence on the time scale does not influence the magnitude agreement of the results. In general, the heat rates and temperature response predicted by both codes is in good agreement.

The material properties of composites represent a source of uncertainty and can lead to different results. The two sets of material properties for graphite epoxy used in this study revealed that the final results can vary between complete survival and complete demise, depending on how the composite is modeled.

As the good agreement is now confirmed for simple shape objects, comparisons with a step-by-step increased level of detail should be carried out because of the still unexplained differences for the results of a complete satellite reentry.

ACKNOWLEDGMENTS

The SCARAB calculations presented in this paper were performed under contract by the German Space Agency DLR and funded by the German Ministry for Education and Technology BMBF under grand number 50JR0481. The authors also wish to acknowledge the excellent cooperation of all parties involved in this study.

REFERENCES

Lips, T. and B. Fritsche, A Comparison of Commonly Used Re-entry Analysis Tool, 55th IAC, Vancouver, Canada, 2004 (soon to be published in *Acta Astronautica*)

Klinkrad, H., and B. Fritsche, Thermal Destruction of Hollow Spheres during Atmospheric Entry - Test Results Computed with the SCARAB S/W System, presented at 16th IADC Meeting, Toulouse, France, 1998

Rochelle, W. C. et al., Results of IAC Reentry Survivability Benchmark Cases: Comparison of NASA ORSAT 5.0 Code with ESA SCARAB Code, presented at 17th IADC Meeting, Darmstadt, Germany, October 1999

Koppenwallner, G., The Drag of Simple Shaped Bodies in Rarefied Hypersonic Flow Regime, AIAA-85-0998, Williamsburg, VA, June 19-21, 1985